Chemical Science

ROYAL SOCIETY OF CHEMISTRY

EDGE ARTICLE

View Article Online
View Journal | View Issue

Cite this: *Chem. Sci.*, 2023, **14**, 6449

All publication charges for this article have been paid for by the Royal Society of Chemistry

Received 14th April 2023
Accepted 19th May 2023

DOI: 10.1039/d3sc01945d

rsc.li/chemical-science

Asymmetric imino-acylation of alkenes enabled by HAT-photo/nickel cocatalysis†

Rui Wang and Chuan Wang *

By merging nickel-mediated facially selective aza-Heck cyclization and radical acyl C–H activation promoted by tetrabutylammonium decatungstate (TBADT) as a hydrogen atom transfer (HAT) photocatalyst, we accomplish an asymmetric imino-acylation of oxime ester-tethered alkenes with readily available aldehydes as the acyl source, enabling the synthesis of highly enantioenriched pyrrolines bearing an acyl-substituted stereogenic center under mild conditions. Preliminary mechanistic studies support a Ni(I)/Ni(II)/Ni(III) catalytic sequence involving the intramolecular migratory insertion of a tethered olefinic unit into the Ni(III)–N bond as the enantiodiscriminating step.

Introduction

Cyclization of oxime derivative-tethered alkenes[1] has emerged as a powerful tool for the synthesis of pyrrolines, which are a characteristic structural motif found in numerous natural products and biologically active compounds.[2] Mechanistically, these ring closure reactions either proceed *via* the transition metal-promoted aza-Heck reaction[3] or are mediated by iminyl radicals under photoredox catalysis.[4] Among various imino-cyclization reactions, imino-acylation of oxime ester-tethered alkenes provides pyrrolines containing a synthetically highly useful carbonyl moiety as the products and thus has attracted considerable attention from synthetic chemists in recent years (Scheme 1A). In 2015, Bower reported a palladium-catalyzed redox-neutral three-component imino-acylation of alkenes incorporating a pendant oxime ester with carbon monoxide and organoborons as coupling partners.[5] In 2019, our group developed a nickel-catalyzed olefin imino-acylation employing acid chlorides or anhydrides as the acylating agent under reductive conditions.[6] Very recently, Zhao[7] and Ye[8] successfully applied redox N-heterocyclic carbene catalysis in diastereoselective olefin imino-acylation using aromatic aldehydes or acyl imidazoles as the acyl source. Despite impressive advances, none of these aforementioned imino-acylation reactions could yield highly enantioenriched products. Therefore, establishing a new mode for asymmetric olefin imino-acylation is still highly desired.

As a hydrogen-atom-transfer (HAT) photocatalyst, tetrabutylammonium decatungstate (TBADT) is able to promote the homolytic cleavage of the acyl C–H bond of aldehydes as well as the aliphatic C–H bond of hydrocarbons, to produce nucleophilic carbon-centered radicals, which can be used as coupling partners with various electrophiles.[9–11] Recently, the scope of C–H functionalization reactions involving TBADT has been significantly expanded through the combination of transition-metal catalysis.[12] We focus our research on the asymmetric variants of these reactions[13] and accomplished enantioselective olefin acyl-carbamoylation[14] and acyl C–H allylation,[15] which are the only two precedents in asymmetric cooperative catalysis of transition

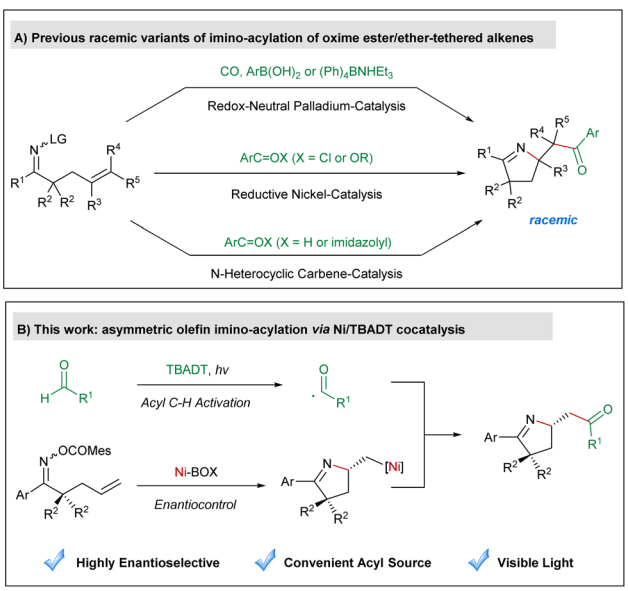

Scheme 1 (A) Previous racemic variants of imino-acylation of oxime ester/ether-tethered alkenes; (B) asymmetric olefin imino-acylation *via* Ni/TBADT cocatalysis.

Hefei National Laboratory for Physical Science at the Microscale, Department of Chemistry, Center for Excellence in Molecular Synthesis, University of Science and Technology of China, 96 Jinzhai Road, Hefei, Anhui 230026, P. R. China. E-mail: chuanw@ustc.edu.cn

† Electronic supplementary information (ESI) available: Experimental procedure, spectral data, NMR-data, and HPLC-data. CCDC 2246373. For ESI and crystallographic data in CIF or other electronic format see DOI: https://doi.org/10.1039/d3sc01945d

metals and TBADT to the best of our knowledge. As a continuation of our ongoing interest in this research area, we herein envision an asymmetric imino-acylation reaction of oxime ester-tethered alkenes with aldehydes through merging nickel-mediated enantioselective aza-Heck cyclization and TBADT-promoted acyl C–H activation, to allow for the synthesis of diverse pyrrolines bearing an acyl-substituted stereogenic center in a highly enantioselective fashion (Scheme 1B). The major challenge of the anticipated transformation lies in the avoidance of iminyl radical-mediated uncontrolled ring closure.

Results and discussion

For optimization of the reaction conditions, we utilized butyraldehyde (**1a**) and the mesitoyl oxime ester **2a** incorporating a terminal olefinic unit as the standard substrates (Table 1). After the systematic screening of various reaction parameters, we identified the optimized reaction conditions as follows: $Ni(ClO_4)_2\cdot 6H_2O$ (15 mol%), the BOX ligand **L1** (18 mol%), TBADT (5 mol%), and $NaClO_4$ (0.5 equiv.) under irradiation at 390 nm for 24 h in MeCN at room temperature. In this case, the desired imino-acylation product **3aa** was obtained in 66% yield and 99% ee (entry 1), wherein the major by-products are the ketone **2a′** (9%) and the hydroimination product **3aa′** (11%, 15% ee). Subsequently, we varied the reaction parameters to demonstrate their influence on the outcome of the target transformation. Only 7% ee could be achieved in the case of the PHOX **L2** as the ligand, which has been proven to be the best ligand in our previously reported Ni/TBADT-cocatalyzed asymmetric reactions[14,15] (entry 2). In the case of the PyBox **L3**, the

Table 1 Deviation of the reaction conditions from the optimized conditions[a]

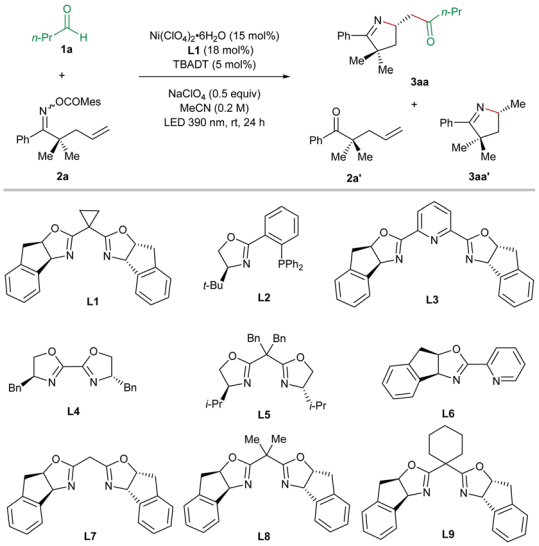

Entry	Deviation from optimized conditions	Yield **3aa**[b] (%)	ee[c] (%)
1	**None**	**66**	**99**
2	**L2** instead of **L1**	78	7
3	**L3** instead of **L1**	40	0
4	**L4** instead of **L1**	65	0
5	**L5** instead of **L1**	26	9
6	**L6** instead of **L1**	70	0
7	**L7** instead of **L1**	62	10
8	**L8** instead of **L1**	47	63
9	**L9** instead of **L1**	73	13
11	NiI_2 instead of $Ni(ClO_4)_2\cdot 6H_2O$	40	96
12	$Ni(BF_4)_2\cdot 6H_2O$ instead of $Ni(ClO_4)_2\cdot 6H_2O$	62	98
13	$NiBr_2\cdot$glyme instead of $Ni(ClO_4)_2\cdot 6H_2O$	33	96
14	$Ni(acac)_2$ instead of $Ni(ClO_4)_2\cdot 6H_2O$	10	94
15	$Ni(cod)_2$ instead of $Ni(ClO_4)_2\cdot 6H_2O$	43	99
16	Acetone instead of MeCN	25	91
17	w/o $NaClO_4$	61	98
18	w/o $Ni(ClO_4)_2\cdot 6H_2O$ or TBADT or light	0	—

[a] Unless otherwise specified, the reactions were performed on a 0.2 mmol scale of the oxime ester **2a** using 3 equiv. of butyraldehyde (**1a**), 15 mol% $Ni(ClO_4)_2\cdot 6H_2O$, 18 mol% ligand **L1**, 5 mol% TBADT, and 0.5 equiv. of $NaClO_4$ in 1 mL MeCN under irradiation at 390 nm for 24 h (two lamps 5 cm away, with adequate fans and a water bath to keep the reaction at room temperature). [b] Yields of isolated products through column chromatography. [c] Determined by HPLC-analysis on a chiral stationary phase.

BiOX **L4**, the BOX **L5**, or the PyrOx **L6**, the imino-acylation reaction proceeded with very poor or no asymmetric induction (entries 3–6). The substitution pattern of the bridging methylene of the BOX ligands turned out to be vital for the enantioselectivity of the studied reaction. Compared to the chiral BOX **L1**, ligands **L7–L9** resulted in substantially lower enantioselectivities (entries 7–9). The use of other nickel precatalysts including NiI_2, $Ni(BF_4)_2 \cdot 6H_2O$, $NiBr_2 \cdot$glyme, $Ni(acac)_2$, and $Ni(cod)_2$ gave rise to inferior results (entries 11–15). Replacing MeCN with acetone as the solvent led to a decrease in both yield and enantiomeric excess of **3aa** (entry 16). Without the addition of $NaClO_4$, both the efficiency and the enantiocontrol of the desired reaction were slightly attenuated (entry 17). In the absence of nickel, TBADT, or irradiation, no desired imino-acylation occurred, confirming their crucial roles in this cooperative catalysis (entry 18).

With the optimized reaction conditions in hand, we started to evaluate the substrate scope of this nickel/photo-cocatalyzed olefin imino-acylation. First, various aldehydes were reacted with the oxime ester-tethered alkene **2a** under standard conditions (Table 2). The aliphatic aldehydes without α-substitution (**1a–1e**) provided the products **3aa–3ea** in moderate to good yields and excellent enantioselectivities.

In the case of bulkier α-branched aldehydes (**1f** and **1g**), the products **3af** and **3ag** were obtained in slightly lower yields while the asymmetric induction remained high. In contrast, the reactions employing α-trisubstituted aldehydes such as pivalaldehyde and 2,2-diphenylpropanal failed to yield the desired products. Subsequently, the generality of aromatic aldehydes for the studied reaction was interrogated. Benzaldehyde (**1h**) and its derivatives bearing either electron-donating or weak electron-withdrawing substitution on the *para*, *meta*, or *ortho* positions of the phenyl ring (**1i–1n** and **1q–1t**) were all found to be pertinent precursors, furnishing the products **3ia–3na** and **3qa–3ta** in a highly enantioselective manner. In contrast, strong electron-withdrawing substituents on the phenyl ring turned out to have a detrimental effect on the enantiocontrol (**3oa** and **3pa**). Furthermore, the naphthaldehydes **1u** and **1v**, as well as the heteroaryl aldehydes bearing a furan (**1w**), thiophene (**1x**), or pyrazole unit (**1y**) were also suitable precursors, providing the corresponding products **3ua–3ya** in high enantiocontrol. In addition, the reaction on a 2 mmol scale of **2a** toward the synthesis of compound **3aa** provided a similar result in terms of both efficiency and asymmetric induction (64% yield, 98% ee).

Next, we continued to explore the substrate scope by varying the structure of the oxime ester-tethered alkenes in the reactions with butyraldehyde (**1a**), and the results are summarized in Table 3. Starting from the cyclic substrates **2b** and **2c**, the highly enantioenriched pyrrolines with a spirocyclic scaffold (**3ab** and **3ac**) were synthesized in excellent enantioselectivity and in 52% and 75% yield, respectively. Unfortunately, the absence of geminal substitution of the linker between oxime ester and alkene led to a dramatic decrease in both efficiency and enantiocontrol (**3ad**). Furthermore, the reaction using the α-monomethyl substituted oxime ester **2e** delivered the imino-acylation product **3ae** in a low diastereomeric ratio and low enantiomeric excesses. In the case of 1,1-disubstituted alkene, a quaternary stereogenic center could be constructed albeit in a relatively low enantiomeric excess (**3af**). Subsequently, the permutation of different substitutions on the phenyl ring of the

Table 2 Evaluation of the substrate scope of aldehydes[a,b,c,d]

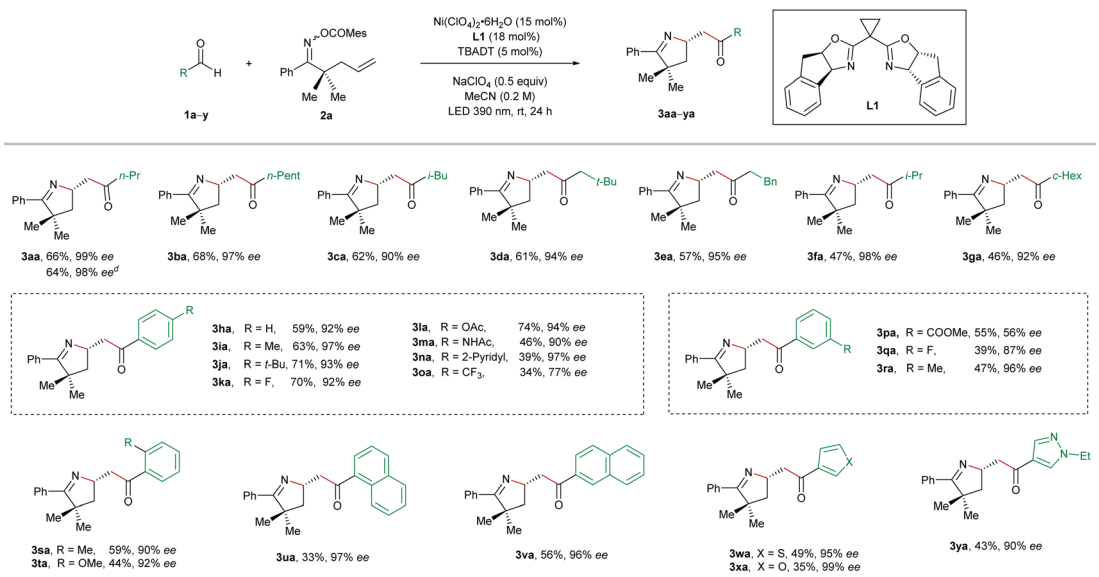

[a] Unless otherwise specified, the reactions were performed on a 0.2 mmol scale of the oxime ester **2a** using 3 equiv. of the aldehydes **1a–1y**, 15 mol% $Ni(ClO_4)_2 \cdot 6H_2O$, 18 mol% ligand **L1**, 5 mol% TBADT, and 0.5 equiv. of $NaClO_4$ in 1 mL MeCN under irradiation at 390 nm for 24 h (two lamps 5 cm away, with adequate fans and a water bath to keep the reaction at room temperature). [b] Yields of the isolated products after column chromatography. [c] Enantiomeric excesses were determined by HPLC-analysis on a chiral stationary phase. [d] The reaction was performed on a 2 mmol scale of the oxime ester **2a**.

Table 3 Evaluation of the substrate scope of oxime-ester-tethered alkenes[a,b,c]

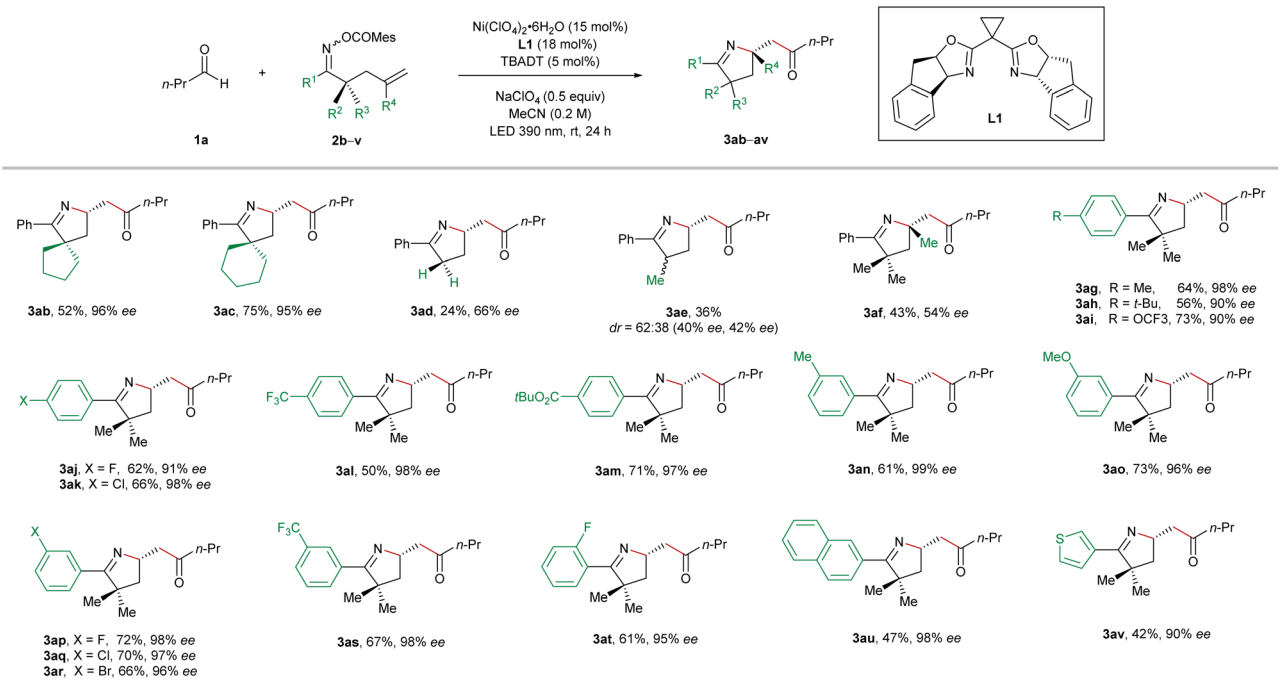

[a] Unless otherwise specified, the reactions were performed on a 0.2 mmol scale of the oxime esters **2b–2v** using 3 equiv. of butyraldehyde (**1a**), 15 mol% $Ni(ClO_4)_2 \cdot 6H_2O$, 18 mol% ligand **L1**, 5 mol% TBADT, and 0.5 equiv. of $NaClO_4$ in 1 mL MeCN under irradiation at 390 nm for 24 h (two lamps 5 cm away, with adequate fans and a water bath to keep the reaction at room temperature). [b] Yields for the isolated products after column chromatography. [c] Enantiomeric excesses were determined by HPLC-analysis on a chiral stationary phase.

oxime esters **2g–2t** was carried out. In general, in the case of both electron-donating and electron-withdrawing substituents, all the reactions proceeded smoothly, furnishing the products **3ag–3at** in moderate to good yields with excellent enantiocontrol. Moreover, the naphthyl and thienyl oxime esters **2u** and **2v** also turned out to be suitable precursors for this cocatalyzed reaction, providing the coupling products **3au** and **3av** in high enantiomeric excesses. Unsuccessful substrates for this reaction include internal olefins and oxime esters derived from dialkyl ketones.

To demonstrate the utility of this method, various derivatizations starting from imino-acylation product **3aa** or **3ha** were carried out (Scheme 2). First, Wittig olefination successfully converted compound **3aa** into a chiral alkene (**4**) in 61% yield and 98% ee. Next, compound **3aa** was reacted with tosylhydrazine to afford a *Z*-configured hydrazone (**5**) in 53% yield and 96% ee, the absolute configuration of which was unambiguously determined to be *S* through X-ray crystallography (CCDC number: 2246373). By means of *m*CPBA-mediated oxidation of compound **3aa**, a chiral oxaziridine (**6**) was obtained as a single diastereomer in 68% yield and 98% ee. Notably, such structural motifs are often used as O- or N-atom transferring agents and the precursors for [3 + 2] cycloadditions.[16] Furthermore, DIBAL-H turned out to be able to promote the chemo- and diastereoselective reduction of the carbonyl group of compound **3aa** in DCM at −78 °C, leading to the formation of a chiral secondary alcohol (**7**) in 54% yield, 98% ee, and >98 : 2 dr. Moreover, treatment of compounds **3aa** and **3ha** with the Grignard reagents provided the corresponding chiral tertiary alcohols **8** (88% yield, 96% ee) and **9** (60% yield, 90% ee), respectively. In addition, the latter was subjected to $NaBH(OAc)_3$-mediated reduction, furnishing a chiral diphenyl homoprolinol (**10**) in 75% yield, 10 : 1 dr, and 92% ee, which might find applications as a catalyst or a catalyst precursor since it is structurally analogous to CBS-[17] and the Jørgensen–Hayashi[18] catalyst.

In order to shed light on the mechanism of this reaction, we carried out a set of control experiments and cyclic voltammetry studies (Scheme 3). Under the standard reaction conditions, the oxime esters bearing benzoate (**2a-1**) or acetate (**2a-2**) as the leaving group were utilized as the precursors instead of mesitoate (**2a**), yielding the product **3aa** in significantly lower enantiomeric excess (Scheme 3A). Subsequently, 1,4-cyclohexadiene was employed instead of butanal in this reaction, and the hydroimination product **3aa′** was afforded in 16% ee (Scheme 3B), which is consistent with the ee of the isolated byproduct in the imino-acylation reaction demonstrated in Table 1. The aforementioned results confirm that the enantiocontrol in the cyclization process depends on both the properties of the leaving group and the presence of an acyl source, indicating that acyl and carboxylate are both probably attached to the nickel center when it performs the enantiodiscriminating intramolecular migratory insertion with the pendant olefin. Moreover, we conducted the reaction between the oxime ester **2a** and butanal (**1a**) under the sole photocatalysis of TBADT (Scheme

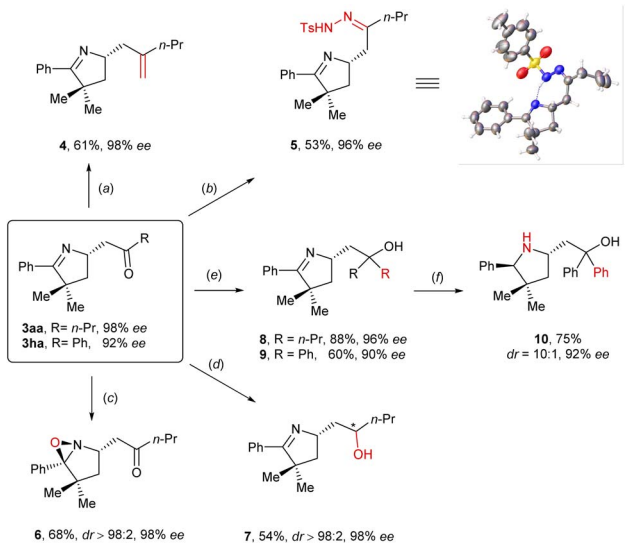

Scheme 2 Derivatizations of imino-acylation products.

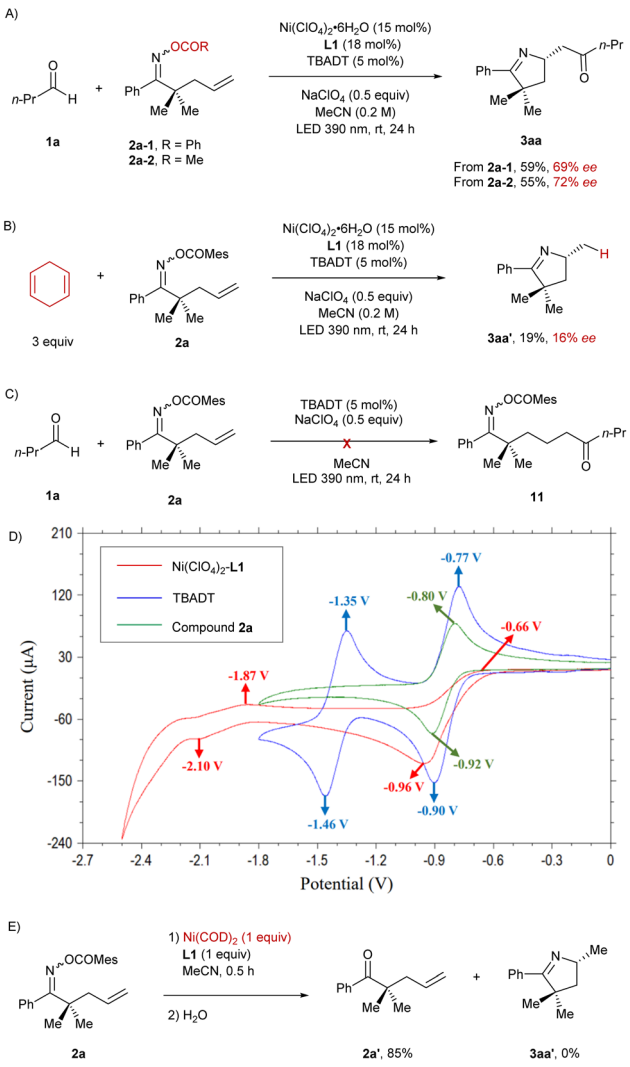

Scheme 3 Control experiments and cyclic voltammetry studies.

3C). No hydroacylation occurred in this case, suggesting that the addition of an acyl radical to the terminal olefinic unit could not serve as an elementary step for the initial C–C bond formation in this cocatalyzed imino-acylation reaction. Cyclic voltammetry studies reveal that the half-wave potential of $[W]^{5-}/[W]^{6-}$ ($E_{1/2} = -1.41$ V *vs.* Ag/AgCl)[19] is more negative than the one of Ni(II)/Ni(I) ($E_{1/2} = -0.81$ V *vs.* Ag/AgCl) but less negative than the one of Ni(I)/Ni(0) ($E_{1/2} = -1.99$ V *vs.* Ag/AgCl) in acetonitrile, indicating that Ni(I) species can be generated *in situ* starting from the Ni(II) precatalyst through reduction by $[W]^{6-}$ (Scheme 3D). Besides, the half-wave potential of the oxime ester **2a** ($E_{1/2} = -0.86$ V *vs.* Ag/AgCl) turned out to be slightly more negative than the one of Ni(II)/Ni(I), accounting for the preferred reduction of Ni(II) by $[W]^{6-}$ in the presence of oxime esters in the reaction mixture. In addition, the stoichiometric reaction of the oxime ester **2a** with the Ni(0) complex generated from $Ni(COD)_2$ and **L1** did not yield any ring closure product, which also argues against the reaction sequence of Ni(0)-mediated oxidative addition followed by Ni(II)-mediated cyclization (Scheme 3E).

On the basis of the results of the preliminary mechanistic investigations, a plausible reaction mechanism exemplified by butyraldehyde (**1a**) and the oxime ester-tethered alkene **2a** is proposed in Scheme 4. Initially, decatungstate $[W]^{4-}$ is activated to $[W]^{4-}$* under irradiation at 390 nm, which subsequently abstracts a hydrogen atom from butyraldehyde (**1a**), leading to the formation of corresponding acyl radical **A** and $[W]^{5-}H^+$. Disproportionation of the latter affords original $[W]^{4-}$ for the next TBADT catalytic cycle and $[W]^{6-}2H^+$, which is able to

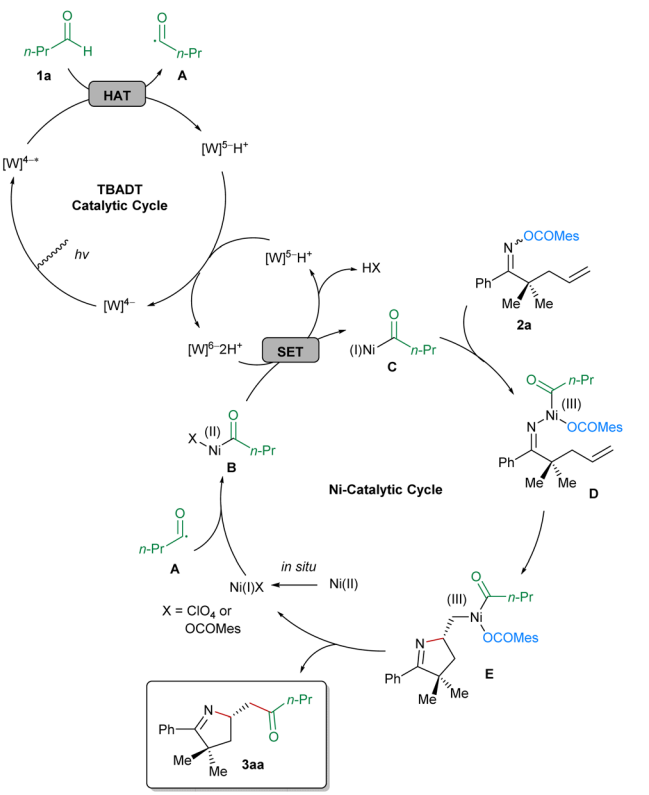

Scheme 4 Proposed reaction mechanism.

reduce Ni(II) to Ni(I) *via* single-electron transfer (SET). In the nickel-catalytic cycle, the *in situ* generated Ni(I) is oxidized by the acyl radical **A**, to provide the acyl-Ni(II) species **B**, which is reduced to the acyl-Ni(I) species **C** by $[W]^{6-}$ $2H^+$ *via* SET. Next, the oxime ester **2a** performs oxidative addition to the Ni(I) complex **C**, to afford the Ni(III) intermediate **D**, the pendant olefinic unit of which undergoes the enantiodetermining migratory insertion into the Ni–N bond. After facile reductive elimination from the resultant Ni(III) complex **E**, the corresponding imino-acylation product **3aa** is furnished and Ni(I) is regenerated for the next catalytic cycle.

Conclusions

In conclusion, we have developed an asymmetric imino-acylation reaction of oxime ester-tethered alkenes with aldehydes, which proceeds under the cooperative catalysis of a nickel-BOX complex and TBADT as a HAT photocatalyst, providing a new method to construct a chiral pyrroline scaffold. The synthetic diversification potential of the imino-acylation products has been demonstrated through various derivatizations based on the chemoselective transformations of the incorporated carbonyl and imino moieties. On the basis of the results of control experiments and cyclic voltammetry, a catalytic cycle with Ni(I) as the initial operating species has been proposed, in which Ni(III)-mediated aza–Heck cyclization serves as the enantiodetermining step.

Data availability

General information, detailed experimental procedures, characterization data for all new compounds, NMR spectra, and HPLC chromatograms are in the ESI.† Data for the crystal structure reported in this paper have been deposited at the Cambridge Crystallographic Data Centre (CCDC) under the deposition number CCDC 2246373.

Author contributions

C. W. designed the project and wrote the paper. R. W. carried out the experimental work. Both authors analyzed the data, discussed the results, and commented on the manuscript.

Conflicts of interest

There is no conflict to declare.

Acknowledgements

This work was supported by the National Natural Science Foundation of China (22071230 and 22271267).

Notes and references

1 For reviews on cyclization of oxime ester-tethered alkenes, see: (*a*) M. Kitamura and K. Narasaka, *Chem. Rec.*, 2002, **2**, 268–277; (*b*) N. J. Race, I. R. Hazelden, A. Faulkner and J. F. Bower, *Chem. Sci.*, 2017, **8**, 5248–5260; (*c*) J. Davies, S. P. Morcillo, J. J. Douglas and D. Leonori, *Chem. Eur J.*, 2018, **24**, 12154–12163; (*d*) C. Chen, J. Zhao, X. Shi, L. Liu, Y.-P. Zhu, W. Sun and B. Zhu, *Org. Chem. Front.*, 2020, **7**, 1948–1969; (*e*) X.-Y. Yu, Q.-Q. Zhao, J. Chen, W.-J. Xiao and J.-R. Chen, *Acc. Chem. Res.*, 2020, **53**, 1066–1083; (*f*) K. Kwon, R. T. Simons, M. Nandakumar and J. L. Roizen, *Chem. Rev.*, 2022, **122**, 2353–2428; (*g*) C. Pratley, S. Fenner and J. A. Murphy, *Chem. Rev.*, 2022, **122**, 8181–8260.

2 (*a*) V. C. Clark, C. J. Raxworthy, V. Rakotomalala, P. Sierwald and B. L. Fisher, *Proc. Natl. Acad. Sci. U. S. A.*, 2005, **102**, 11617–11622; (*b*) A. Adams and N. De Kimpe, *Chem. Rev.*, 2006, **106**, 2299–2319; (*c*) E. Vitaku, D. T. Smith and J. T. Njadarson, *J. Med. Chem.*, 2014, **57**, 10257–10274; (*d*) F. Bellina and R. Rossi, *Tetrahedron*, 2006, **62**, 7213–7256.

3 For selected examples of transition metal-catalyzed aza-Heck cyclization using oxime-tethered alkenes, see: (*a*) H. Tsutsui and K. Narasaka, *Chem. Lett.*, 1999, **28**, 45–46; (*b*) Y. Koganemaru, M. Kitamura and K. Narasaki, *Chem. Lett.*, 2002, **31**, 784–785; (*c*) A. Faulkner and J. F. Bower, *Angew. Chem., Int. Ed.*, 2012, **51**, 1675–1679; (*d*) A. Faulkner, N. J. Race, J. S. Scott and J. F. Bower, *Chem. Sci.*, 2014, **5**, 2416–2421; (*e*) B. C. Lemercier and J. G. Pierce, *Org. Lett.*, 2014, **16**, 2074–2076; (*f*) C. Chen, L. Hou, M. Cheng, J. Su and X. Tong, *Angew. Chem., Int. Ed.*, 2015, **54**, 3092–3096; (*g*) H. Su, W. Li, Z. Xuan and W. Yu, *Adv. Synth. Catal.*, 2015, **357**, 64–70; (*h*) N. J. Race, A. Faulkner, M. H. Shaw and J. F. Bower, *Chem. Sci.*, 2016, **7**, 1508–1513; (*i*) N. J. Race, A. Faulkner, G. Fumagalli, T. Yamauchi, J. S. Scott, M. Rydén-Landergren, S. A. Sparkes and J. F. Bower, *Chem. Sci.*, 2017, **8**, 1981–1985; (*j*) X. Bao, Q. Wang and J. Zhu, *Angew. Chem., Int. Ed.*, 2017, **56**, 9577–9581; (*k*) H.-B. Yang, S. R. Pathipati and N. Selander, *ACS Catal.*, 2017, **7**, 8441–8445; (*l*) T. Shimbayashi, K. Okamoto and K. Ohe, *Chem.–Asian J.*, 2018, **13**, 395–399; (*m*) L. Wang and C. Wang, *J. Org. Chem.*, 2019, **84**, 6547–6556; (*n*) Y. Zhang and X.-F. Wu, *Chem. Commun.*, 2020, **56**, 14605–14608; (*o*) L. Feng, L. Guo, C. Yang, J. Zhou and W. Xia, *Org. Lett.*, 2020, **22**, 3964–3968; (*p*) Y. Zhang, H.-J. Ai and X.-F. Wu, *Org. Chem. Front.*, 2020, **7**, 2986–2990; (*q*) W.-X. Wei, Y. Li, Y.-T. Wen, M. Li, X.-S. Li, C.-T. Wang, H.-C. Liu, Y. Xia, B.-S. Zhang, R.-Q. Jiao and Y.-M. Liang, *J. Am. Chem. Soc.*, 2021, **143**, 7868–7875; (*r*) X.-G. Jia, Q.-W. Yao and X.-Z. Shu, *J. Am. Chem. Soc.*, 2022, **144**, 13461–13467; (*s*) D. Qi, X. Zhang, X. Wang, X. Liu, Z. Zhang, L. Shi and G. Zhang, *Org. Lett.*, 2023, **25**, 1126–1130.

4 For selected examples of photo-catalyzed cyclization using oxime-tethered alkenes, see: (*a*) T. Mikami and K. Narasaka, *Chem. Lett.*, 2000, **29**, 338–339; (*b*) H. Jiang, X. An, K. Tong, T. Zheng, Y. Zhang and S. Yu, *Angew. Chem., Int. Ed.*, 2015, **54**, 4055–4059; (*c*) J. Davies, S. J. Booth, S. Essafi, R. A. W. Dryfe and D. Leonori, *Angew. Chem., Int. Ed.*, 2015, **54**, 14017–14021; (*d*) S.-H. Cai, J.-H. Xie, S. Song, L. Ye, C. Feng and T.-P. Loh, *ACS Catal.*, 2016, **6**, 5571–5574; (*e*) H. Jiang and A. Studer, *Angew. Chem., Int. Ed.*, 2017, **56**, 12273–12276; (*f*) J. Davies,

N. S. Sheikh and D. Leonori, *Angew. Chem., Int. Ed.*, 2017, **56**, 13361–13365; (*g*) K. M. Nakafuku, S. C. Fosu and D. A. Nagib, *J. Am. Chem. Soc.*, 2018, **140**, 11202–11205; (*h*) X. Shen, C. Huang, X.-A. Yuan and S. Yu, *Angew. Chem., Int. Ed.*, 2021, **60**, 9672–9679; (*i*) A. F. Prusinowski, H. C. Sise, T. N. Bednar and D. A. Nagib, *ACS Catal.*, 2022, **12**, 4327–4332.

5 A. Faulkner, J. S. Scott and J. F. Bower, *J. Am. Chem. Soc.*, 2015, **137**, 7224–7230.

6 L. Wang and C. Wang, *Org. Chem. Front.*, 2018, **5**, 3476–3482.

7 W.-D. Liu, W. Lee, H. Shu, C. Xiao, H. Xu, X. Chen, K. N. Houk and J. Zhao, *J. Am. Chem. Soc.*, 2022, **144**, 22767–22777.

8 Y.-X. Dong, C.-L. Zhang, Z.-H. Gao and S. Ye, *Org. Lett.*, 2023, **25**, 855–860.

9 For reviews of TBADT-catalyzed reactions, see: (*a*) C. L. Hill, *Synlett*, 1995, **1995**, 127–132; (*b*) M. D. Tzirakis, I. N. Lykakis and M. Orfanopoulos, *Chem. Soc. Rev.*, 2009, **38**, 2609–2621; (*c*) D. Ravelli, S. Protti and M. Fagnoni, *Acc. Chem. Res.*, 2016, **49**, 2232–2242; (*d*) D. Ravelli, M. Fagnoni, T. Fukuyama, T. Nishikawa and I. Ryu, *ACS Catal.*, 2018, **8**, 701–713; (*e*) X. Yuan, G. Yang and B. Yu, *Chin. J. Org. Chem.*, 2020, **40**, 3620–3632; (*f*) L. Capaldo, D. Ravelli and M. Fagnoni, *Chem. Rev.*, 2022, **122**, 1875–1924; (*g*) H. Cao, X. Tang, H. Tang, Y. Yuan and J. Wu, *Chem Catal.*, 2021, **1**, 523–598.

10 For selected examples of TBADT-catalyzed acyl C–H activation reactions of aldehydes, see: (*a*) S. Esposti, D. Dondi, M. Fagnoni and A. Albini, *Angew. Chem., Int. Ed.*, 2007, **46**, 2531–2534; (*b*) M. D. Tziraki and M. Orfanopoulos, *J. Am. Chem. Soc.*, 2009, **131**, 4063–4069; (*c*) D. Ravelli, S. Montanaro, M. Zema, M. Fagnoni and A. Albini, *Adv. Synth. Catal.*, 2011, **353**, 3295–3300; (*d*) I. Ryu, A. Tani, T. Fukuyama, D. Ravelli, S. Montanaro and M. Fagnoni, *Org. Lett.*, 2013, **15**, 2554–2557; (*e*) F. Bonassi, D. Ravelli, S. Protti and M. Fagnoni, *Adv. Synth. Catal.*, 2015, **357**, 3687–3695; (*f*) L. Capaldo, M. Fagnoni and D. Ravelli, *Chem. Eur J.*, 2017, **23**, 6527–6530; (*g*) P. Fan, C. Zhang, Y. Lan, Z. Lin, L. Zhang and C. Wang, *Chem. Commun.*, 2019, **55**, 12691–12694; (*h*) J. Dong, X. Wang, Z. Wang, H. Song, Y. Liu and Q. Wang, *Chem. Sci.*, 2020, **11**, 1026–1031; (*i*) Y. Kuang, H. Cao, H. Tang, J. Chew, W. Chen, X. Shi and J. Wu, *Chem. Sci.*, 2020, **11**, 8912–8918; (*j*) J. Dong, F. Yue, X. Wang, H. Song, Y. Liu and Q. Wang, *Org. Lett.*, 2020, **22**, 8272–8277; (*k*) A. Prieto and M. Taillefer, *Org. Lett.*, 2021, **23**, 1484–1488; (*l*) X. Wang, Y. Chen, H. Song, Y. Liu and Q. Wang, *Org. Lett.*, 2021, **23**, 2199–2204; (*m*) S. Le, J. Li, J. Feng, Z. Zhang, Y. Bai, Z. Yuan and G. Zhu, *Nat. Commun.*, 2022, **13**, 4734; (*n*) Y. Mao, P. Fan and C. Wang, *Org. Lett.*, 2022, **24**, 9413–9418; (*o*) T. Varlet, D. Bouchet, E. van Eslande and G. Masson, *Chem. Eur J.*, 2022, **28**, e202201707.

11 For selected examples of TBADT-catalyzed aliphatic C–H activation reactions of hydrocarbons, see: (*a*) D. Dondi, M. Fagnoni, A. Molinari, A. Maldotti and A. Albini, *Chem. Eur J.*, 2004, **10**, 142–148; (*b*) D. Dondi, M. Fagnoni and A. Albini, *Chem. Eur J.*, 2006, **12**, 4153–4163; (*c*) M. D. Tzirakis and M. Orfanopoulos, *Org. Lett.*, 2008, **10**, 873–876; (*d*) D. Ravelli, A. Albini and M. Fagnoni, *Chem. Eur J.*, 2011, **17**, 572–579; (*e*) S. D. Halparin, H. Fan, S. Chang, R. E. Martin and R. Britton, *Angew. Chem., Int. Ed.*, 2014, **53**, 4690–4693; (*f*) M. Okada, T. Fukuyama, K. Yamada, I. Ryu, D. Ravelli and M. Fagnoni, *Chem. Sci.*, 2014, **5**, 2893–2898; (*g*) D. Ravelli, M. Zoccolillo, M. Mella and M. Fagnoni, *Adv. Synth. Catal.*, 2014, **356**, 2781–2786; (*h*) J. J. Murphy, D. Bastida, S. Paria, M. Fagnoni and P. Melchiorre, *Nature*, 2016, **532**, 218–222; (*i*) V. I. Supranovich, V. V. Levin and A. D. Dilman, *Org. Lett.*, 2019, **21**, 4271–4274; (*j*) K. Yahata, S. Sakurai, S. Hori, S. Yoshioka, K. Hasegawa and S. Akai, *Org. Lett.*, 2020, **22**, 1199–1203; (*k*) G. Laudadio, Y. Deng, K. van der Wal, D. Ravelli, M. Nuño, M. Fagnoni, D. Guthrie, Y. Sun and T. Noël, *Science*, 2020, **369**, 92–96; (*l*) P. J. Sarver, N. B. Bissonnette and D. W. C. MacMillan, *J. Am. Chem. Soc.*, 2021, **143**, 9737–9743; (*m*) L. Capaldo and D. Ravelli, *Org. Lett.*, 2021, **23**, 2243–2247; (*n*) T. E. Schirmer, A. B. Rolka, T. A. Karl, F. Holzhausen and B. König, *Org. Lett.*, 2021, **23**, 5729–5733; (*o*) Q. Liu, Y. Ding, Y. Gao, Y. Yang, L. Gao, Z. Pan and C. Xia, *Org. Lett.*, 2022, **24**, 7983–7987.

12 For selected examples of transition metal/TBADT-cocatalyzed reactions, see: (*a*) I. B. Perry, T. F. Brewer, P. J. Sarver, D. M. Schultz, D. A. DiRocco and D. W. C. MacMillan, *Nature*, 2018, **560**, 70–75; (*b*) P. J. Sarver, V. Bacauanu, D. M. Shultz, D. A. DiRocco, Y.-h. Lam, E. C. Sherer and D. W. C. MacMillan, *Nat. Chem.*, 2020, **12**, 459–467; (*c*) H. Cao, Y. Kuang, X. Shi, K. L. Wong, B. B. Tan, J. M. C. Kwan, X. Liu and J. Wu, *Nat. Commun.*, 2020, **11**, 1956; (*d*) L. Wang, T. Wang, G.-J. Cheng, X. Li, J.-J. Wei, B. Guo, C. Zheng, G. Chen, C. Ran and C. Zheng, *ACS Catal.*, 2020, **10**, 7543–7551; (*e*) P. Fan, C. Zhang, L. Zhang and C. Wang, *Org. Lett.*, 2020, **22**, 3875–3878; (*f*) S. Xu, H. Chen, J. Zhu and W. Kong, *Angew. Chem., Int. Ed.*, 2021, **60**, 7405–7411; (*g*) P. Fan, Y. Jin, J. Liu, R. Wang and C. Wang, *Org. Lett.*, 2021, **23**, 7364–7369; (*h*) P. Fan, R. Wang and C. Wang, *Org. Lett.*, 2021, **23**, 7672–7677; (*i*) V. Murugesan, A. Ganguly, A. Karthika and R. Rasappan, *Org. Lett.*, 2021, **23**, 5389–5393; (*j*) D. Mazzarella, A. Pulcinella, L. Bovy, R. Broersma and T. Noël, *Angew. Chem., Int. Ed.*, 2021, **60**, 21277–21282; (*k*) B. Maity, C. Zhu, M. Rueping and L. Cavallo, *ACS Catal.*, 2021, **11**, 13973–13982; (*l*) D. Wang and L. Ackermann, *Chem. Sci.*, 2022, **13**, 7256–7263; (*m*) Y. Jin, E. W. H. Ng, T. Fan, H. Hirao and L.-Z. Gong, *ACS Catal.*, 2022, **12**, 10039–10046; (*n*) W. Liu, C. Liu, M. Wang and W. Kong, *ACS Catal.*, 2022, **12**, 10207–10221; (*o*) Q. Wang, S. Ni, L. Yu, Y. Pan and Y. Wang, *ACS Catal.*, 2022, **12**, 11071–11077; (*p*) P. Fan, Y. Mao and C. Wang, *Org. Chem. Front.*, 2022, **9**, 4649–4653; (*q*) W. Liu, Y. Ke, C. Liu and W. Kong, *Chem. Commun.*, 2022, **58**, 11937–11940; (*r*) X. Li, Y. Mao, P. Fan and C. Wang, *Eur. J. Org. Chem.*, 2022, **2022**, e202200214; (*s*) V. Murugesan, A. Muralidharan, G. V. Anantharaj, T. Chinusamy and R. Rasappan, *Org. Lett.*, 2022, **24**, 8435–8440; (*t*) E. Mao and D. W. C. MacMillan, *J. Am. Chem. Soc.*, 2023, **145**, 2787–2793.

13 For reviews on asymmetric transition metal/photo cocatalysis, see: (*a*) X. Huang and E. Meggers, *Acc. Chem. Res.*, 2019, **52**, 833–847; (*b*) C. Jiang, W. Chen, W.-H. Zheng and H. Lu, *Org. Biomol. Chem.*, 2019, **17**, 8673–8689; (*c*) H. H. Zhang, H. Chen, C. Zhu and S. Yu, *Sci. China Chem.*, 2020, **63**, 637–647; (*d*) A. Lipp, S. O. Badir and G. A. Molander, *Angew. Chem., Int. Ed.*, 2021, **60**, 1714–1726; (*e*) Y. Li, Z. Ye, J. Cai and L. Gong, *Synthesis*, 2021, **53**, 1570–1583; (*f*) F.-D. Lu, J. Chen, X. Jiang, J.-R. Chen, L.-Q. Lu and W.-J. Xiao, *Chem. Soc. Rev.*, 2021, **50**, 12808–12827; (*g*) Z. Li, C. Li, Y. Ding and H. Huo, *Coord. Chem. Rev.*, 2022, **460**, 214479; (*h*) A. Y. Chan, I. B. Perry, N. B. Bissonnette, B. F. Buksh, G. A. Edwards, L. I. Frye, O. L. Garry, M. N. Lavagnino, B. X. Li, Y. Liang, E. Mao, A. Millet, J. V. Oakley, N. L. Reed, H. A. Sakai, C. P. Seath and D. W. C. MacMillan, *Chem. Rev.*, 2022, **122**, 1485–1542.

14 P. Fan, Y. Lan, C. Zhang and C. Wang, *J. Am. Chem. Soc.*, 2020, **142**, 2180–2186.

15 R. Wang, P. Fan and C. Wang, *ACS Catal.*, 2023, **13**, 141–146.

16 K. S. Williamson, D. J. Michaelis and T. P. Yoon, *Chem. Rev.*, 2014, **114**, 8016–8036.

17 C. J. Helal and M. P. Meyer, The Corey–Bakshi–Shibata reduction: mechanistic and synthetic considerations – bifunctional Lewis base catalysis with dual activation, in *Lewis Base Catalysis in Organic Synthesis*, Wiley, Hoboken, 2016, ch. 11, pp. 387–389.

18 K. L. Jensen, G. Dickmeiss, H. Jiang, Ł. Albrecht and K. A. Jørgensen, *Acc. Chem. Res.*, 2012, **45**, 248–264.

19 T. Yamase, N. Tapakayashi and M. Kaji, *J. Chem. Soc., Dalton Trans.*, 1984, 793–799.